The *Arabidopsis dnd1* "defense, no death" gene encodes a mutated cyclic nucleotide-gated ion channel

Steven J. Clough*†, Kevin A. Fengler*†‡, I-ching Yu*§, Bernadette Lippok*¶, Roger K. Smith, Jr.‖††, and Andrew F. Bent*‖**††‡‡**

*Department of Crop Sciences and ‖Physiological and Molecular Plant Biology Program, University of Illinois at Urbana-Champaign, Urbana, IL 61801; and **Department of Plant Pathology, University of Wisconsin at Madison, Madison, WI 53706

Edited by Frederick M. Ausubel, Harvard Medical School, Boston, MA, and approved May 23, 2000 (received for review January 6, 2000)

Gene-for-gene disease resistance typically includes a programmed cell death response known as the hypersensitive response (HR). The *Arabidopsis thaliana dnd1* mutant was previously isolated as a line that failed to produce the HR in response to avirulent *Pseudomonas syringae* pathogens; plants homozygous for the recessive *dnd1-1* mutation still carry out effective gene-for-gene resistance. The *dnd1-1* mutation also causes constitutive systemic resistance and elevated levels of salicylic acid. In the present study, a positional cloning approach was used to isolate *DND1*. *DND1* encodes the same protein as AtCNGC2, a cyclic nucleotide-gated ion channel of previously unknown organismal function that can allow passage of Ca^{2+}, K^+ and other cations [Leng, Q., Mercier, R. W., Yao, W. & Berkowitz, G. A. (1999) *Plant Physiol.* 121, 753–761]. By using a nahG transgene, we found that salicylic acid is required for the elevated resistance caused by the *dnd1* mutation but that removal of salicylic acid did not completely eliminate the dwarf and loss-of-HR phenotypes of mutant *dnd1* plants. A stop codon that would severely truncate the *DND1* gene product was identified in the *dnd1-1* allele. This demonstrates that broad-spectrum disease resistance and inhibition of the HR can be activated in plants by disruption of a cyclic nucleotide-gated ion channel.

Gene-for-gene disease resistance in plants is characterized by specific recognition of certain pathogens and is controlled by plant resistance genes and pathogen avirulence genes with corresponding specificity (1, 2). The ensuing highly effective defense response typically includes the hypersensitive response (HR), a programmed cell death process in host cells immediately adjacent to the pathogen (3, 4). The HR apparently contributes to disease resistance by fostering release of antimicrobial enzymes and metabolites, by physically isolating the pathogen within defined lesions, and/or by enhancing local and systemic signaling to activate defenses in non-infected cells. However, cell death itself is not essential to limit pathogen growth. Many types of disease resistance do not involve HR cell death, and, even within gene-for-gene resistance, examples have emerged in which cell death is not essential (ref. 5 and references therein). For example, strong alleles of the *Rx* gene in potato condition resistance to Potato Virus X without activation of the HR (6, 7) whereas mutant *ndr1* plants exhibit an HR-like response to some avirulent *Pseudomonas syringae* yet are disease-susceptible (8).

Systemic acquired resistance is a broad-spectrum form of disease resistance in which prior infection or immunizing treatment causes systemic activation of some defense responses and potentiation of subsequent responsiveness to pathogens (9–11). Systemic acquired resistance can confer varying levels of resistance against many different (but not all) viral, bacterial, and fungal plant pathogens. Salicylic acid and the *NPR1* (*NIM1*) gene product are key mediators of systemic acquired resistance as well as gene-for-gene disease resistance. Additional defense activation pathways exist that are independent of salicylic acid (9, 10).

The *dnd* (defense, no death) class of mutants, including *dnd1*, *dnd2*, and Y15, were identified by their reduced ability to produce the HR in response to avirulent *Pseudomonas syringae* pv. *glycinea* (*Psg*) and were isolated in a screen designed to discover additional components of the *avrRpt2-RPS2* disease resistance pathway in *Arabidopsis* (5, 12). The *dnd1* mutant provides an example of gene-for-gene resistance without the HR. Despite the virtual absence of HR cell death, *dnd1* mutants retain defense responses characteristic of gene-for-gene resistance such as strong induction of pathogenesis-related gene expression and the ability to severely limit pathogen growth (5). Interestingly, *dnd1* plants also exhibit quantitative systemic acquired resistance-like resistance to a variety of virulent bacterial, fungal, and viral pathogens, and are dwarfed in stature. This broad-spectrum resistance and dwarfing was likely to be attributable in part to the constitutive elevation of salicylic acid compounds observed in *dnd1* plants, as similar phenomena have been observed in other *Arabidopsis* elevated-salicylate mutants (13). However, the loss-of-HR phenotype of *dnd1* plants is unusual among characterized *Arabidopsis* mutants that display elevated salicylic acid levels (13, 14).

Some of the earliest detectable signaling events in plant defense responses include transmembrane ion fluxes (influx of Ca^{2+} and H^+ and efflux of K^+ and Cl^-) and the production of reactive oxygen species such as superoxide and hydrogen peroxide (15–17). For example, physiological changes in membrane permeability are observed in parsley suspension cells between 2 and 5 min after treatment with a fungal elicitor (18). Resistant cowpea plants display an elevated level of cytosolic Ca^{2+} in infected epidermal cells whereas susceptible plants do not (19). Ca^{2+} channel blockers have been shown to inhibit HR in tobacco and soybean systems (20–23). Ca^{2+} channel blockers also disrupt other defense responses to fungal and bacterial elicitors (21, 24,

This paper was submitted directly (Track II) to the PNAS office.

Abbreviations: HR, hypersensitive response; BAC, bacterial artificial chromosome; CNG, cyclic nucleotide-gated.

Data deposition: The sequence reported in this paper has been deposited in the GenBank database (accession no. AF280939).

†S.J.C. and K.A.F. contributed equally to this paper.

‡Present address: Dupont Agricultural Biotechnology, Delaware Technology Park, Newark, DE 19714.

§Present address: Department of Biology, University of North Carolina, Chapel Hill, NC 27599.

¶Present address: Max Plank Institut für Züchtungforschung, D-50829 Köln, Germany.

††Present address: Department of Plant Pathology, University of Wisconsin at Madison, Madison, WI 53706.

‡‡To whom reprint requests should be addressed. E-mail: afb@plantpath.wisc.edu.

The publication costs of this article were defrayed in part by page charge payment. This article must therefore be hereby marked "*advertisement*" in accordance with 18 U.S.C. §1734 solely to indicate this fact.

Article published online before print: *Proc. Natl. Acad. Sci. USA*, 10.1073/pnas.150005697. Article and publication date are at www.pnas.org/cgi/doi/10.1073/pnas.150005697

25). Ion fluxes are thought to be required for the activation of a mitogen-activated protein kinase, specific to defense responses, that may serve to activate gene expression after its translocation to the nucleus (26). Significantly, Ca^{2+} influx and the transient increase in cytosolic Ca^{2+} levels after elicitor treatment have been shown to be necessary and sufficient for the induction of the oxidative burst (27). Although these and numerous other studies have implicated ion fluxes in plant defense signaling (16, 28, 29), genetically based systems implicating ion channels in defense activation have not been available.

In the present study, we report the cloning and initial characterization of *Arabidopsis DND1*, which was found to encode a cyclic nucleotide-gated ion channel. We also report evidence suggesting that salicylic acid is required for the elevated disease resistance but not the suppression of HR in *dnd1* mutants.

Materials and Methods

High-Resolution Genetic Mapping. Previously described restriction fragment length polymorphism markers (www.arabidopsis.org/) or bacterial artificial chromosome-derived cosmids (see below) were used to probe survey filters carrying restriction enzyme digests of Col-0 and No-0 genomic DNA. DNA of individuals from a Col-0 *dnd1-1/dnd1-1* × No-0 F2 population that were known to carry recombination events between CHS1 and nga106 was digested, blotted, and probed to determine genotypes at these marker loci. The *DND1* genotype of these individuals was determined by plant size and by HR testing, as described (5). Standard recombinant DNA methods (30) were used in these and all other experiments unless specifically noted.

BAC Identification and Alignment. To identify BAC clones spanning the region of interest, a filter carrying the TAMU (Texas A&M University) *Arabidopsis* BAC library (*Arabidopsis* Biological Resource Center, Columbus, OH) was probed with markers pCIT1243 and nga106. pCIT1243 hybridized to TAMU BAC clone 21I05 and the Washington University BAC fingerprinting database indicated close similarity between 21I05 and IGF clone 1L1 (31). Similarly, nga106 identified IGF clone 5E1. These data oriented with respect to the genome a previously non-anchored contig from the IGF BAC contig database that contained 1L1 and 5E1 (32). The four BACs 8M21, 3H2, 22L1, and 23B17 were then selected from the IGF contig database as representatives of the relevant genomic region and were obtained from the *Arabidopsis* Biological Resource Center.

Creation and Mapping of Binary Cosmid Library. To create a library competent for *Agrobacterium*-mediated plant transformation and spanning the putative *DND1* locus, DNA of BACs 8M21, 3H2, 22L1, and 23B17 was isolated, was further purified by cesium chloride gradient, was partially digested with Sau3A to produce a predominance of 15- to 25-kb DNA fragments, was dephosphorylated with shrimp alkaline phosphatase, and then was ligated into the *Bam*HI site of cesium chloride-purified binary/cosmid vector pCLD04541 (33). Ligation products were packaged as phage and were transfected into *Escherichia coli* XL1-Blue-MR by using the Gigapack III XL kit (Stratagene). Colonies were selected and purified on LB medium with tetracycline (10 μg/ml) and were stored at −60°C in 96-well microtiter plates. To determine overlap between cosmids and to allow for rough mapping with respect to the source BAC clones, cosmids were fingerprinted with restriction enzymes unique to the vector polylinker, and unique cosmids were double-digested with *Eco*RI and *Xba*I and blotted to nylon membrane along with single-enzyme digested BAC DNA. Blots were probed with select cosmids that were ^{32}P-labeled. pBeLoBAC (BAC vector) DNA was used to probe cosmid blots to identify cosmid subclones that contained vector DNA.

Functional Complementation of the *dnd1* Phenotype. Cosmid clones spanning BACs 8M21, 3H2, 22L1, and 23B17 were moved into *Agrobacterium tumefaciens* GV3101(MP90) (34) by electroporation or by tri-parental mating, and were used to transform *Arabidopsis dnd1/dnd1* mutants via the floral dip method (35). After selection for 7–10 days on kanamycin media, primary transformants were transplanted to soil and were grown for an additional ≈4 weeks, at which time the rosette sizes of individual transformants were compared with those of kanamycin-resistant Col-0 controls that were similarly selected on kanamycin plates and transplanted to soil. T_2 seeds for subsequent analysis were collected after self-fertilization of these primary (T_1) transformants.

Bacterial Growth and HR Experiments. Growth of bacterial populations within leaves was determined by vacuum infiltration of 5×10^4 colony-forming units/ml *P. syringae* pv. *tomato* DC3000 (*Pst* DC3000) carrying either *avrRpt2* (pV288) or no *avr* gene (pVSP61, vector only), leaf sampling, and plating on selective media, as described (5). Ability to produce the HR was tested as described (5) by hand inoculation of three leaves on each plant using an OD_{600} = 0.2 suspension (≈2×10^8 colony-forming units/ml) of *P. syringae* pv. *glycinea* Race 4 (*Psg* R4) carrying *avrRpt2*; an additional leaf was inoculated with *Psg* R4 (pVSP61) as a control. The severity of HR was rated on a 0–5 scale (0 = no visible tissue collapse; 5 = total collapse of infiltrated area).

Subcloning, Complementation, and Sequencing. Complementing cosmids were restriction mapped by using sites unique to the pCDL04541 polylinker (*Cla*I, *Pst*I, *Xho*I, and *Hin*dIII). Targeted fragments were subcloned into pBluescript II SK(+) (Stratagene) for DNA sequencing and/or into pCDL04541 for complementation analysis as described above. At least five putative *Arabidopsis* transformants of a *dnd1/dnd1* line were obtained for most subclones. DNA sequencing was performed by using the BigDye Terminator Kit (PE Biosystems), M13 Forward and Reverse primers, and an ABI377 sequencing apparatus. Sequence data were analyzed by using Sequencher (Genes Code, Ann Arbor, MI) and publicly available BLAST programs (www.ncbi.nlm.nih.gov). To sequence the *dnd1-1* mutant allele, the primers 5′-TCTAGAGAAGTCCGTCCATCGAA-3′ and 5′-TCTAGAGCGATCTTTGAGGTTTGCTC-3′ were used along with *Pfu* Turbo DNA polymerase (Stratagene) to isolate a 5.3-kb PCR product from the Col-0 *dnd1-1/dnd1-1* line. PCR products were directly sequenced by using additional primers internal to the *DND1* gene. The single base difference between *DND1* and *dnd1-1* was confirmed by sequencing the relevant region of four independent PCR products.

Construction of *dnd1 nahG*$^+$ Lines. *Arabidopsis* Col-0 carrying the well characterized "B15" transgene insertion event of *nahG*$^+$ under control of a ^{35}S promoter was kindly provided by CIBA–Geigy/Novartis (Research Triangle Park, NC). A Ler-0 line carrying a similar construct with a different *nahG* gene was kindly provided by Xinnian Dong (Duke University, Durham, NC). Both lines were crossed to Col-0 *dnd1-1/dnd1-1*, and, for each cross, two separate experimental lines were derived by self-fertilization of F_2 segregants homozygous for *dnd1-1* and the *nahG*$^+$ construct.

DNA Blot Analysis. Total genomic DNA from a variety of plant species was restricted with *Hin*dIII and *Eco*RI (single-enzyme digests), was separated by agarose gel electrophoresis, and was blotted and probed with a ^{32}P-labeled version of the 5.3-kb *DND1* PCR product described above or a full-length AtCNGC2 cDNA clone pAtCNGC2wt (kindly provided by of R. Mercier and G. Berkowitz, University of Connecticut, Storrs, CT).

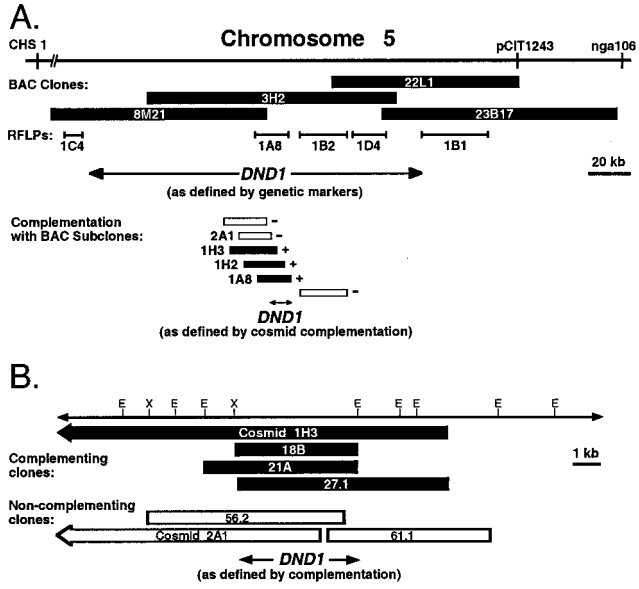

Fig. 1. Summary of positional cloning experiments leading to isolation of the *DND1* gene. (*A*) CHS1, pCIT1243, and nga106 are previously mapped molecular genetic markers on *Arabidopsis* chromosome 5. pCIT1243 and nga106 were used to identify BAC clones carrying wild-type Col-0 genomic DNA inserts. Inserts from four BACs were subcloned to create a binary cosmid library; some of these cosmids were used as additional restriction fragment length polymorphism markers to refine the genetic interval containing *DND1*. Three cosmids that complement the *dnd1* mutation were identified of 43 tested in a focused shotgun complementation project. (*B*) Higher-resolution complementation experiments using more precise subclones identified additional complementing and noncomplementing clones, including other clones not shown, that implicated an ≈5-kb region as the *DND1* locus. This region encodes a previously identified cDNA named AtCNGC2. Cosmids 1H3 and 2A1 are shown in both *A* and *B*. E, *Eco*RI site; X, *Xba*I site.

Fig. 2. Size-complementation of mutant *dnd1* plants by addition of the cloned wild-type *DND1* locus. Col-0 *dnd1-1*/*dnd1-1* plants transformed with cosmids 1A8 or 1H2, or other complementing cosmids (not shown), corrected the *dnd1* dwarf rosette phenotype.

Results

Positional Cloning of *DND1*. The *dnd1* phenotypes are caused by a single locus recessive mutation in lines homozygous for the EMS-induced *dnd1-1* mutant allele (5). Mapping with a population of 536 F_2 individuals from a No-0 × Col *dnd1-1*/*dnd1-1* cross had localized the *dnd1* mutation to the genetic interval between markers CHS1 and nga106 on chromosome 5. The HR^- and dwarf phenotypes were 100% linked (5). In the present study, we used a positional cloning approach to isolate and characterize the *DND1* gene.

Initial efforts focused on identification of additional polymorphic markers in the CHS1-nga106 region. By using previously mapped markers, *DND1* was placed between pCIT1243 (0.3 cM away) and CHS1 (1.3 cM away; see Fig. 1*A*).

Arabidopsis Col-0 genomic DNA BAC clones 8M21, 3H2, 22L1, and 23B17 were identified as optimally representing this region (Fig. 1*A*; see *Materials and Methods*). These BACs were then subcloned as 15- to 25-kb fragments in a transformation-competent binary vector. Restriction digest fingerprinting and hybridization to blots carrying restricted BAC DNA revealed that these subclone libraries were composed of at least 27, 29, 18, and 7 unique cosmid clones for 8M21, 3H2, 22L1, and 23B17, respectively, and that they provided substantial representation of the region of interest (data not shown).

The BAC-derived binary cosmid sublibrary facilitated further high-resolution mapping efforts. New restriction fragment length polymorphism markers were developed from five cosmids polymorphic between Col-0 and No-0. Cosmids 1C4 and 1B1 flanked informative recombination events from the mapping population whereas cosmids 1A8, 1B2, and 1D4 absolutely cosegregated with *DND1* (Fig. 1*A*). Cosmids 1C4 and 1B1 defined a physical interval of roughly 150 kb spanning the *DND1* locus.

A focused shotgun complementation strategy was pursued for identification of *DND1* while the above mapping was in progress. Mutant *dnd1* plants were transformed with individual cosmids from the BAC sublibraries, and primary transformants were then screened for reversion of the dwarf phenotype. As mapping proceeded, particular emphasis was placed on cosmids representing the region flanked by markers 1C4 and 1B1. For unknown reasons possibly related to the constitutive broad-spectrum resistance phenotype, *dnd1* plants exhibited a low transformation rate relative to wild-type Col-0 (≈0.05% transformants per total number of seeds tested compared with ≈1% for Col-0). Although we generated transformants for only 43 cosmids across the contig, this was sufficient as T_1 plants from cosmids 1A8 (BAC 3H2), 1H2 (BAC 3H2), and 1H3 (BAC 3H2) appeared to be complemented ($n = 2$ for each). These plants exhibited sizes similar to wild-type controls (Fig. 2; data not shown). These three cosmids all mapped physically to the same region of BAC 3H2 and displayed a high degree of overlap (Fig. 1*A*). T_2 plants from each of the complemented lines segregated approximately 3:1 for size, reflecting the hemizygous nature of the T-DNA in the primary transformants (wild-type:dwarf segregation ratios = 23:6 for 1A8, 32:10 for 1H2, and 29:13 for 1H3). None of the transformants carrying the other 40 BAC-derived cosmids complemented the *dnd1* mutation (Fig. 1*A*; data not shown). The region carrying the *DND1* gene was delimited to approximately 10 kb by these positive and negative complementation results (Fig. 1*A*).

Identification of the *DND1* Gene. Once complementing cosmids were identified, overlapping subclones from these cosmids were generated for precise gene identification by further complementation tests and DNA sequencing. By using a variety of restriction enzymes (see *Materials and Methods*), 0.6- to 9-kb fragments were subcloned in parallel into the binary vector pCLD04541 and into pBluescript II SK(+). Transformants of the *dnd1* line were obtained for 14 subclones, and these transformants were examined for size complementation. Rosette size was quantified for these transformants, and significant differences from non-complemented *dnd1* controls were observed for some clones (Fig. 1*B*; data not shown). Identification of overlapping clones that complemented or failed to complement the *dnd1* mutation

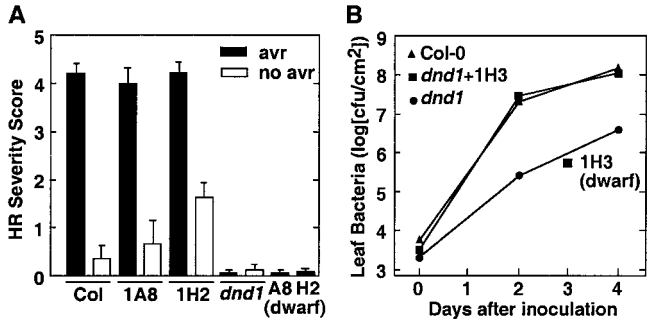

Fig. 3. Complementation of the reduced-HR and constitutive resistance phenotypes of *dnd1* plants by transformation with cloned wild-type *DND1*. (*A*) HR scores for leaves inoculated with *P. syringae* pv. *glycinea* Race 4 carrying cloned *avrRpt2* (filled bars) or an empty plasmid vector (open bars). HR tissue collapse scored on a scale of 0–5 (0 = no visible collapse; 5 = confluent collapse of inoculated tissue; values are mean ± SE). Data are shown for T_2 plants derived from hemizygous primary transformants; 1A8 (dwarf) and 1H2 (dwarf) represent control sets of T_2 segregants that returned to the *dnd1*/*dnd1* dwarf rosette size because of loss (via segregation) of the *DND1* transgene. (*B*) Growth of virulent *P. syringae* pv. *tomato* DC3000 in leaf tissue of inoculated plants. Col-0, wild type; 1H3, Col-0 *dnd1*/*dnd1* line carrying wild-type *DND1* because of transformation with cosmid 1H3; *dnd1*, Col-0 *dnd1*/*dnd1*; 1H3 (dwarf), dwarf-sized T_2 plants from a Col-0 *dnd1*/*dnd1* T_1 transformant that was hemizygous for the introduced 1H3 construct.

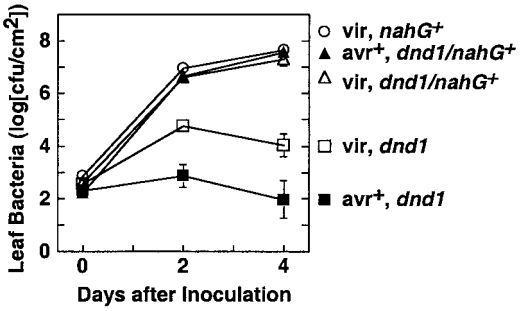

Fig. 4. Loss of resistance in salicylate hydroxylase plants. Leaves were inoculated uniformly with virulent *P. syringae* pv. *tomato* DC3000 (open symbols) or *Pst* DC3000 *avrRpt2*$^+$ (filled symbols). Squares, Col-0 *dnd1*/*dnd1* line; circles, Col-0 *nahG*$^+$ B15 line; triangles, Col-0 *dnd1*/*dnd1*, *nahG*$^+$/*nahG*$^+$ line. Leaf population data are shown as mean ± SE.

suggested that *DND1* resides partially or completely on a single 5.2-kb *Eco*RI/*Xba*I fragment (Fig. 1*B*).

After initially monitoring complementation of the dwarf phenotype, complementation of defense-related *dnd1* phenotypes was confirmed in assays of HR tissue collapse and of resistance to virulent *P. syringae*. A strong HR was observed in response to *P. syringae* expressing *avrRpt2* in T_2 progeny of *dnd1* lines that carried size-complementing transgene constructs whereas dwarf T_2 segregants from the same hemizygous T_1 parent retained the *dnd1* HR$^-$ phenotype (Fig. 3*A*; data not shown). The constitutive resistance phenotype of mutant *dnd1* plants was also eliminated (reverted to the wild-type phenotype) by complementation with the putative wild-type *DND1* gene (Fig. 3*B*).

Determination of the DNA sequence of the *dnd1* complementing region and adjacent sequences from noncomplementing clones (GenBank accession number AF280939) revealed eight 83- to 675-bp stretches of sequence with 100% identity to the recently released nucleotide sequence of cDNA AtCNGC2 (GenBank accession nos. Y16328 and AF067798; refs. 36 and 37). These regions of identity, together with the intervening sequences that do not match AtCNGC2, reveal the intron/exon structure of a 3,327-bp *DND1* gene composed of eight exons. The full-length AtCNGC2 cDNA, isolated independently by Köhler and Neuhaus (36) and Leng *et al.* (37), spans all but a 1.85-kb region at one end of the genomic segment defined by our complementing and noncomplementing subclones (Fig. 1*B*). No significant database matches or extensive open reading frames were observed in this non-AtCNGC2 region, and our clones 2A1 and 56.2 carried this genomic region but failed to complement the *dnd1* mutation (Fig. 1*B*). These data indicate that *DND1* encodes the AtCNGC2 cDNA. The derived DND1/AtCNGC2 amino acid sequence bears regions of similarity to animal cyclic nucleotide-gated ion channels, and AtCNGC2 has been shown to encode a functional cyclic nucleotide-gated ion channel (refs. 37 and 38; see *Discussion*).

The DNA sequence of the *dnd1-1* mutant allele was determined to further test the above conclusions and to examine the nature of this defense-altering mutation. One base-change was detected in a region spanning the *dnd1-1* gene as well as 1.4 kb of putative upstream controlling sequence and 400 bp of downstream sequence. The *dnd1-1* allele contains a G to A point mutation that creates a stop codon in exon 3 at Trp_{290} (amino acid no. 290 of 720 total), presumably creating a severely truncated DND1 protein.

Depletion of Salicylic Acid. Previous work had determined that mutant *dnd1* plants produce elevated levels of free- and glucoside-conjugated salicylic acid (5). To place the *dnd1* mutation with respect to salicylate-mediated defense signaling pathways, we constructed plant lines homozygous for the *dnd1-1* mutation and expressing *nahG*, a bacterial salicylate hydroxylase gene that causes depletion of salicylate levels (39). Expression of *nahG* disrupted both the elevated partial resistance against the normally virulent pathogen *P. syringae* pv. *tomato* DC3000 and the gene-for-gene resistance elicited in response to *Pst* DC3000 expressing *avrRpt2* (Fig. 4). Similar loss of resistance was observed with other separately constructed *dnd1*/*dnd1 nahG*$^+$ lines (data not shown).

Despite the strong impact on disease resistance, other *dnd1* phenotypes were not fully reverted to wild-type by removal of salicylic acid. The *dnd1*/*dnd1 nahG*$^+$ lines reproducibly grew with a "semidwarf" leaf and rosette size that was intermediate between wild-type and the dwarfed *dnd1*/*dnd1*plants. The loss-of-HR phenotype of *dnd1* mutants also remained in *dnd1*/*dnd1 nahG*$^+$ plants. Depletion of SA by *nahG* has been previously reported to disrupt the HR (40). In wild-type plants carrying *nahG*$^+$, we found that the HR was not entirely abolished but, rather, was delayed such that tissue collapse was evident 48 h rather than 24 h after high-titer inoculation with *Psg* R4 carrying *avrRpt2* (Table 1). However, in *dnd1*/*dnd1 nahG*$^+$ lines, we

Table 1. HR in plant lines depleted of salicylic acid by expression of *nahG*

	24 hr		48 hr	
Plant line*	*avrRpt2*$^+$	no *avr*	*avrRpt2*$^+$	no *avr*
Col-0	H5†	H0	H5	H0.5
dnd1	H0	H0	H0	H0
nahG	H0.5	H0	H5	H2
dnd1 + *nahG*‡	H0	H0	H0.1	H0

*Plant lines wild-type Col-0 or Col-0 homozygous for *nahG*$^+$ transgene and/or *dnd1-1* mutation.

†H, average HR severity, scored on 0–5 scale (H0 = no HR; H5 = confluent collapse), after inoculation with 10^8 colony-forming units/ml *Psg* R4 carrying pV288 or pVSP61.

‡Data pooled for four independent lines.

observed that no HR developed, even at 48 h after inoculation (Table 1).

***DND1* in Other Plant Species.** To examine the occurrence of *DND1* homologues in crop species, genomic DNA blots were probed with *Arabidopsis DND1* gene probes. When a cDNA clone was used as probe and blots were washed at moderate stringency (5 × SSC/65°C or 1 × SSC/65°C), only bands corresponding to the known *DND1* genomic locus were observed in *Arabidopsis* samples (data not shown). A single weakly hybridizing band was observed in *Brassica napus* and radish but not other species (listed below). Use of a cDNA clone was important because, in blots probed with labeled genomic *DND1* (containing coding region, ≈1.4 kb of promoter and ≈0.4 kb of 3′ sequence) and washed at high stringency (0.1 × SSC, 65°C), discrete hybridizing bands were clearly present in DNA from soybean, potato, tomato, tobacco, alfalfa, radish, *B. napus*, rice, maize, and oats (data not shown).

Conditional Lesion Mimicry in *dnd1* Plants. In earlier work with non-inoculated *dnd1* mutant plants grown in a variety of environments in the U.S. and U.K., no substantive leaf flecking, necrotic spotting, or other lesion-mimic phenotypes were observed upon inspection by naked eye or in microscopic studies using autofluorescence or trypan blue staining (5). However, in our new laboratory facilities at University of Wisconsin, we observed leaf lesions in some batches of non-inoculated *dnd1* plants. These lesions were pinpoint in size (≈10–50 dead cells) and did not enlarge or coalesce after initial formation. Lesions did not form on control Col-0 plants grown in parallel. Lesion formation was associated with growth of young plants at light intensities of ≈250 $\mu E/m^2$ at low relative humidity in a rapid-drying soil mix, but the vast majority of *dnd1* plants (including plants grown under similar conditions) have not exhibited lesions. Some but not all colleagues working with *dnd1* plants at other locations have also observed lesions. *Arabidopsis dnd1-1/dnd1-1* apparently can be classified as a rare/conditional lesion-mimic line.

Discussion

In an effort to understand the resistance induction and HR-suppression phenotypes of mutant *dnd1* plants, we sought to molecularly characterize the *Arabidopsis DND1* gene. A positional cloning effort identified overlapping genomic DNA subclones from the *DND1* locus that, when transformed into *dnd1/dnd1* plants, cause reversion from dwarf to wild-type rosette size, recovery of the HR, and loss of the constitutive resistance to virulent *P. syringae*. DNA sequencing revealed that *DND1* encodes a cyclic nucleotide-gated ion channel identical to the product of AtCNGC2, a characterized cDNA of previously unknown organismal function (36, 37). The *dnd1-1* mutant allele carries a single nucleotide change that causes a premature stop codon within the *DND1*/AtCNGC2 sequence.

Cyclic nucleotide-gated (CNG) ion channels are very well known from studies of animal systems, where they play central roles in visual and olfactory signal transduction (41, 42). Although CNG ion channels have many structural similarities to voltage-gated ion channels, they are gated primarily by binding of a cytoplasmic ligand (cAMP or cGMP) rather than by voltage. The channels are semiselective cation channels that allow permeation of Ca^{2+}, K^+, Na^+, and other ions, but, in the more well studied examples, their primary physiological activity is to allow movement of Ca^{2+} into cells. CNG ion channels have a characteristic structure in which a cytoplasmic amino terminus is followed by six membrane-spanning domains and a cytoplasmic carboxyl terminus of substantial length (200+ amino acids) that carries the cyclic nucleotide binding domain. Upon multimer formation, a pore-forming domain is apparently formed by characteristic amino acid sequences between the fifth and sixth membrane-spanning domains. Some of these CNG ion channels also carry a calmodulin-binding domain within their amino terminus and can be regulated by intracellular Ca^{2+} levels (41–43).

AtCNGC2 was recently identified by two separate groups via searches of the *Arabidopsis* EST database (44) for entries with similarity to animal cyclic nucleotide-gated ion channels; recovery of homologous full-length cDNA clones yielded AtCNGC2 (36, 37). Köhler *et al.* identified six apparent cyclic nucleotide-gated ion channel genes from *Arabidopsis* (38) and more such genes are present in the *Arabidopsis* genome, but the *DND1*/AtCNGC2 derived amino acid sequence is only 42–43% similar to most of these other genes. Intriguingly, AtCNGC1, -2, -3, and -4 are unlike previously described CNG channels in that they carry a putative calmodulin-binding domain within their carboxyl terminus at a location that physically overlaps the putative cyclic nucleotide binding domain. Yeast two-hybrid experiments were used to document physical interaction between *Arabidopsis* calmodulins and a carboxyl-terminal AtCNGC2 construct (38). Complementation of a yeast K^+-uptake mutant by AtCNGC2 was found to depend on supplementation with membrane-permeable cAMP or cGMP (37). Importantly, voltage clamp analysis using transfected *Xenopus* oocytes or human embryonic kidney cells demonstrated that AtCNGC2 fosters Ca^{2+} and K^+ influx in a cyclic nucleotide-dependent fashion (37). This was the first functional demonstration of a CNG ion channel from plants.

Based on the above findings, we hypothesize that *DND1* encodes a functional cyclic nucleotide-gated ion channel. The defense-altering *dnd1* mutation is recessive (5), and it creates a stop codon before the pore-forming domain between the fifth and sixth putative membrane-spanning domains of AtCNGC2. These findings make it less likely that *dnd1* phenotypes are caused by a leaky or misfunctional channel and suggest instead that the *dnd1* mutation causes a complete absence of functional AtCNGC2 ion channels.

The *dnd1* mutation apparently acts upstream of salicylic acid, as transformation of *dnd1* mutants with *nahG*$^+$ (salicylate hydroxylase) substantially removed the constitutive-resistance of *dnd1* mutants. However, the loss-of-HR and dwarf rosette phenotypes of *dnd1* mutants were not entirely corrected by *nahG*$^+$. Preliminary studies indicated that SA levels were reduced to the limits of detection in *dnd1/dnd1 nahG*$^+$ lines (I-c.Y., K.A.F., S. Sharma, D. Klessig, and A.F.B., unpublished work), implying that the dwarfing and loss-of-HR caused by the *dnd1* mutation are elicited at least in part via salicylate-independent pathways. The responsiveness of wild-type DND1/AtCNGC2 protein to cyclic nucleotides and calmodulin implies that some aspects of DND1 channel regulation lay downstream of phenomena that alter levels cyclic nucleotides and Ca^{2+}.

A number of testable models can be proposed to explain how genetically recessive absence of an ion channel might activate constitutive broad-spectrum resistance or cause disruption of HR cell death. Ca^{2+} influx is a critical early step in defense activation processes (discussed in the introduction), and *DND1* may encode channels that participate directly in pathogen-induced Ca^{2+} influx. However, a straightforward universal requirement of DND1 channels for defense activation is unlikely. Although HR cell death is blocked, defense processes proceed and in fact are potentiated in *dnd1* plants.

It is challenging to build models that explain the simultaneous activation of defenses and loss of HR in mutant *dnd1* plants. It may be that a number of defense responses are constitutively activated in *dnd1* mutants and that among these responses is an elevation of HR-blocking cellular protection processes such as elevated levels of catalase, glutathione *S*-transferase, or ascorbate peroxidase. Defense activation may arise because absence of the DND1 channel alters normal levels of specific ions,

mimicking defense-inducing physiological states. For example, if *DND1* is an inward-rectifying K^+ channel, it is possible that the reduced ability of *dnd1* plants to take up K^+ mimics the ionic environment observed during early stages of infection by pathogens (in which K^+ efflux leads to lower than normal intracellular K^+ concentrations; refs. 3 and 20), producing constitutive defense signaling and constitutive systemic resistance. Wild-type DND1 may function in homeostasis, reestablishing ionic balance after defense activation and/or other stimuli.

It is also possible that the defense-altering phenotypes of *dnd1* plants are the product of unrelated processes precipitated by loss of *DND1*: i.e., that the wild-type DND1/AtCNGC2 ion channel normally functions in processes that have little or no direct relationship to plant defense responses. However, even an indirect relationship between DND1 and defense signaling does not alter the fact that defenses are significantly altered in the *dnd1* mutant. Our work demonstrates that perturbation of a specific CNG ion channel can activate broad-spectrum disease resistance and can perturb HR cell death in higher plants.

The *dnd1* plants are of interest as a starting point for further examination of cell death and defense activation events. For example, Heo *et al.* have recently demonstrated the participation of specific calmodulin isoforms in the activation of defense responses (45), and it would be of interest to examine calmodulin-related defense signaling with respect to *DND1*. Work from both plant and animal systems has focused attention on the relationships between cyclic nucleotides, calcium signaling, ion channel activation, generation of nitric oxide and reactive oxygen species, and the activation of apoptotic cell death and disease resistance (46–50). Plants mutated at *DND1* may be well suited for additional biochemical and genetic studies that address these topics.

A large volume of previous work has generated evidence for the participation of ion fluxes in defense activation or has suggested that these ion fluxes represent important stages in pathogen-induced host cell necrosis or in HR cell death (16, 17, 28). Much of the more precise defense signal transduction work involving ion fluxes has been performed by using isolated plant cells and/or pharmacological approaches. Work with a genetic component has typically exploited genotypes that alter disease resistance rather than genotypes that directly control ion fluxes. Study of *dnd1* has provided a line of evidence for the involvement of ion channels in defense activation, providing a genetic system in which direct perturbation of an ion channel profoundly influences plant disease resistance.

We thank Novartis Corporation and Xinnian Dong for sharing *nahG*$^+$ *Arabidopsis* lines and R. Mercier and G. Berkowitz for the gift of an AtCNGC2 cDNA clone. This work was supported in part by grants from the U.S. Department of Agriculture/National Research Initiative Competitive Grants Program (Plant Pathology) and the National Institute of General Medical Sciences (National Institutes of Health), and a departmental graduate fellowship to K.A.F. sponsored by Pioneer Hi-Bred International, Inc.

1. Hammond-Kosack, K. E. & Jones, J. D. G. (1997) *Annu. Rev. Plant Mol. Biol.* **48,** 575–607.
2. Martin, G. B. (1999) *Curr. Opin. Plant Biol.* **2,** 273–279.
3. Goodman, R. N. & Novacky, A. J. (1994) *The Hypersensitive Reaction in Plants to Pathogens: A Resistance Phenomenon* (Am. Phytopathol. Soc., St. Paul, MN).
4. Richberg, M. H., Aviv, D. H. & Dangl, J. L. (1998) *Curr. Opin. Plant Biol.* **1,** 480–485.
5. Yu, I-c., Parker, J. & Bent, A. F. (1998) *Proc. Natl. Acad. Sci. USA* **95,** 7819–7824.
6. Kohm, B. A., Goulden, M. G., Gilbert, J. E., Kavanagh, T. A. & Baulcombe, D. C. (1993) *Plant Cell* **5,** 913–920.
7. Bendahmane, A., Kanyuka, K. & Baulcombe, D. C. (1999) *Plant Cell* **11,** 781–791.
8. Century, K. S., Holub, E. B. & Staskawicz, B. J. (1995) *Proc. Natl. Acad. Sci. USA* **92,** 6597–6601.
9. Yang, Y., Shah, J. & Klessig, D. F. (1997) *Genes Dev.* **11,** 1621–1639.
10. Glazebrook, J. (1999) *Curr. Opin. Plant Biol.* **2,** 280–286.
11. Ryals, J. L., Neuenschwander, U. H., Willits, M. C., Molina, A., Steiner, H.-Y. & Hunt, M. D. (1996) *Plant Cell* **8,** 1809–1819.
12. Yu, I-c., Fengler, K. A., Clough, S. J. & Bent, A. F. (2000) *Mol. Plant–Microbe Interact.* **13,** 277–286.
13. Greenberg, J. T. (1997) *Annu. Rev. Plant Physiol. Plant Mol. Biol.* **48,** 525–545.
14. Rate, D. N., Cuenca, J. V., Bowman, G. R., Guttman, D. S. & Greenberg, J. T. (1999) *Plant Cell* **11,** 1695–1708.
15. Lamb, C. & Dixon, R. A. (1997) *Annu. Rev. Plant Physiol. Plant Mol. Biol.* **48,** 251–275.
16. Scheel, D. (1998) *Curr. Opin. Plant Biol.* **1,** 305–310.
17. Hammond-Kosack, K. E. & Jones, J. D. G. (1996) *Plant Cell* **8,** 1773–1791.
18. Hahlbrock, K., Scheel, D., Logemenn, E., Nurnberger, T., Papniske, M., Reinhold, S., Sacks, W. R. & Schmelzer, E. (1995) *Proc. Natl. Acad. Sci. USA* **92,** 4150–4157.
19. Xu, H. & Heath, M. C. (1998) *Plant Cell* **9,** 249–259.
20. Atkinson, M. M., Keppler, L. D., Orlandi, E. W., Baker, C. J. & Mischke, C. F. (1990) *Plant Physiol.* **92,** 215–221.
21. Atkinson, M. M., Midland, S. L., Sims, J. J. & Keen, N. T. (1996) *Plant Physiol.* **112,** 297–302.
22. He, S.-Y., Huang, H.-C. & Collmer, A. (1993) *Cell* **73,** 1255–1266.
23. Levine, A., Pennell, R. I., Alvarez, M. E., Palmer, R. & Lamb, C. (1996) *Curr. Biol.* **6,** 427–437.
24. Nurnberger, T., Nennstiel, D., Jabs, T., Sacks, W. R., Hahlbrock, K. & Scheel, D. (1994) *Cell* **78,** 449–460.
25. Romeis, T., Piedras, P., Zhang, S., Klessig, D. F., Hirt, H. & Jones, J. D. (1999) *Plant Cell* **11,** 273–287.
26. Ligternik, W., Kroj, T., zur Neiden, U., Hirt, H. & Scheel, D. (1997) *Science* **276,** 2054–2057.
27. Jabs, T., Tschöpe, M., Colling, C., Hahlbrock, K. & Scheel, D. (1997) *Proc. Natl. Acad. Sci. USA* **94,** 4800–4805.
28. Ebel, J. & Scheel, D. (1997) in *The Mycota, Vol. V: Plant Relationships, Part A* (Springer, Berlin), pp. 85–105.
29. Gabriel, D. & Rolfe, B. (1990) *Annu. Rev. Phytopathol.* **28,** 365–391.
30. Ausubel, F. M., Brent, R., Kingston, R. E., Moore, D. D., Seidman, J. G., Smith, J. A. & Struhl, K. (1997) *Current Protocols In Molecular Biology* (Wiley, New York).
31. Marra, M., Kucaba, T., Sekhon, M., Hillier, L., Martienssen, R., Chinwalla, A., Crockett, J., Fedele, J., Grover, H., Gund, C., *et al.* (1999) *Nat. Genet.* **22,** 265–270.
32. Mozo, T., Fischer, S., Meier-Ewert, S., Lehrach, H. & Altmann, T. (1998) *Plant J.* **16,** 377–384.
33. Bancroft, I., Love, K., Bent, E., Sherson, S., Lister, C., Cobett, C., Goodman, H. M. & Dean, C. (1997) *Weeds World* **4,** 1–9.
34. Koncz, C. & Schell, J. (1986) *Mol. Gen. Genet.* **204,** 383–396.
35. Clough, S. J. & Bent, A. F. (1998) *Plant J.* **16,** 735–743.
36. Köhler, C. & Neuhaus, G. (1998) *Plant Physiol.* **116,** 1604.
37. Leng, Q., Mercier, R. W., Yao, W. & Berkowitz, G. A. (1999) *Plant Physiol.* **121,** 753–761.
38. Köhler, C., Merkle, T. & Neuhaus, G. (1999) *Plant J.* **18,** 97–104.
39. Gaffney, T., Friedrich, L., Vernooij, B., Negrotto, D., Nye, G., Uknes, S., Ward, E., Kessmann, H. & Ward, J. (1993) *Science* **261,** 754–756.
40. Delaney, T. P., Uknes, S., Vernooij, B., Friedrich, L., Weymann, K., Negrotto, D., Gaffney, T., Gutrella, M., Kessmann, H., Ward, E., *et al.* (1994) *Science* **266,** 1247–1250.
41. Zagotta, W. N. & Siegelbaum, S. A. (1996) *Annu. Rev. Neurosci.* **19,** 235–263.
42. Broillet, M. C. & Firestein, S. (1999) *Ann. N.Y. Acad. Sci.* **868,** 730–740.
43. Zielinski, R. E. (1998) *Annu. Rev. Plant Physiol.* **49,** 697–725.
44. Newman, T., de Bruijn, F. J., Green, P., Keegstra, K., Kende, H., McIntosh, L., Ohlrogge, J., Raikhel, N., Somerville, S., Thomashow, M., *et al.* (1994) *Plant Physiol.* **106,** 1241–1255.
45. Heo, W. D., Lee, S. H., Kim, J. C., Chung, W. S., Chun, H. J., Lee, K. J., Park, H. C., Park, C. Y., Choi, J. Y. & Cho, M. J. (1999) *Proc. Natl. Acad. Sci. USA* **96,** 766–771.
46. Delledonne, M., Xia, Y., Dixon, R. A. & Lamb, C. (1998) *Nature (London)* **394,** 585–588.
47. Durner, J., Wendehenne, D. & Klessig, D. F. (1998) *Proc. Natl. Acad. Sci. USA* **95,** 10328–10333.
48. Mason, R. P., Leeds, P. R., Jacob, R. F., Hough, C. J., Zhang, K. G., Mason, P. E. & Chuang, D. M. (1999) *J. Neurochem.* **72,** 1448–1456.
49. Schmid-Antomarchi, H., Schmid-Alliana, A., Romey, G., Ventura, M. A., Breittmayer, V., Millet, M. A., Husson, H., Moghrabi, B., Lazdunski, M. & Rossi, B. (1997) *J. Immunol.* **159,** 6209–6215.
50. Alvarez, M. E., Pennell, R. W., Meijer, P.-J., Ishikawa, A., Dixon, R. A. & Lamb, C. (1998) *Cell* **92,** 773–784.